Polymer Chemistry

Accepted Manuscript

This article can be cited before page numbers have been issued, to do this please use: S. Yoon and B. Chen, *Polym. Chem.*, 2018, DOI: 10.1039/C8PY00544C.

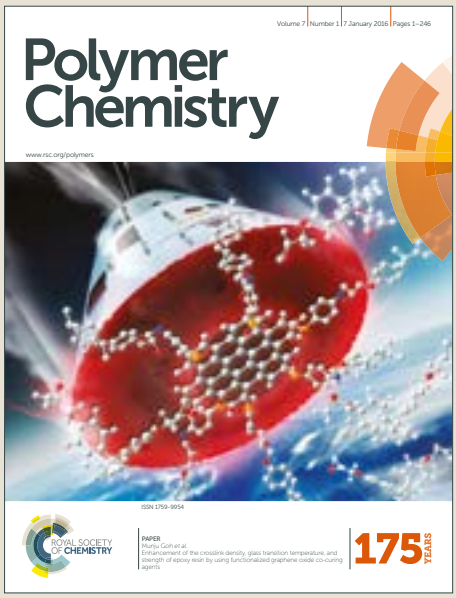

ROYAL SOCIETY OF CHEMISTRY

rsc.li/polymers

View Article Online
DOI: 10.1039/C8PY00544C

Journal Name

ARTICLE

Elastomeric and pH-responsive hydrogels based on direct crosslinking of poly(glycerol sebacate) pre-polymer and gelatin

Received 00th January 20xx,
Accepted 00th January 20xx

DOI: 10.1039/x0xx00000x

www.rsc.org/

Sungkwon Yoon [ab] and Biqiong Chen *[a]

Hydrogels capable of responding to physicochemical dynamics *in vivo* are of significant interest in a variety of advanced biomedical applications. Herein, we develop novel fully biodegradable, biocompatible, highly elastomeric and pH-responsive copolymer hydrogels by direct crosslinking of poly(glycerol sebacate) (PGS) pre-polymer and gelatin *via* their inherent functional groups without the use of any crosslinking agents. The addition of hydrophilic gelatin into the hydrophobic PGS enables the design of hydrogels with both elastomeric properties and water swelling capability as well as pH-responsive behaviours. The copolymer hydrogels were highly flexible and stretchable, enduring complex deformations such as stretching and knotting. Their Young's moduli were in the range of 0.16–0.62 MPa, mimicking the values of some soft tissues. A three-dimensional tissue scaffold with interconnected pore structures was also fabricated which shows full shape recovery after compression further demonstrating high potential of these copolymers to be used in soft tissue engineering applications. The pH-responsive swelling ratios of the copolymer hydrogels were found to be up to 11-fold difference in acidic and basic environments, which resulted in pH-dependent release profiles of a model drug. Moreover, a tunable biodegradation kinetics with an ultimate full degradation in 11 weeks *in vitro* and good cytocompatibility in cell metabolic assay with mouse fibroblasts were also achieved with these copolymer hydrogels. The versatile multifunctionalities in these new copolymer hydrogels illustrate their great potential in soft tissue engineering and controlled drug delivery.

1 Introduction

Hydrogels are of great interest in biotechnology, with their biomimetic macromolecular network structure and soft mechanical property, as well as the high water content that allows the diffusion of desired chemical species.[1–5] A critical aspect in designing hydrogels with advanced functionalities is their interaction with biology. The complex physicochemical dynamics *in vivo* drive the need for developing hydrogels which are capable of responding to biological conditions and stimuli. For instance, hydrogels with elastomeric mechanical property are great assets for soft tissue engineering applications, with their ability to provide biomimetic and synchronous deformations responding to the mechanical dynamics in native tissues.[6] Another example is the stimuli-responsive property. Various *in vivo* stimuli such as water, temperature, mechanical stress, pH, ionic strength, and specific chemical species have been extensively investigated in developing hydrogels with their ability to alter the diffusion characteristics for controlled drug delivery.[2,7–11] Multifunctional hydrogels which are capable of responding to the various biological dynamics, therefore, are an important class of biomaterials for different biomedical applications such as soft tissue engineering and drug delivery.

Poly(glycerol sebacate) (PGS) is a synthetic polyester.[12] Its excellent elastomeric mechanical behaviour resulted from the macromolecular network structure, as well as good biocompatibility with minimal inflammatory responses have attracted much attention in soft tissue engineering such as adipose,[13] cardiac,[14–16] cartilage,[17,18] nerve,[19] retinal,[20,21] and vascular applications.[22–24] PGS also shows surface-erodible biodegradation with a linear weight loss and good strength retention, which is beneficial for long-term implantations in the body and controlled release of functional molecules incorporated within the polymer matrix.[25,26] While its mechanical properties are tunable by altering the synthesis mechanism[27], molar ratio of monomers[28,29], and synthetic conditions such as the reaction time and temperature[16,28–31], PGS has poor hydration property. In spite of the hydroxyl and carboxyl pendant group present on its polymer backbone, it does not swell in water to form swollen hydrogels owing to the aliphatic carbon chains from the sebacic acid monomer. The hydrophobicity of PGS was shown by a low equilibrium water uptake capacity of 2.1 ± 0.9 wt.%,[32] and high water contact

[a] School of Mechanical and Aerospace Engineering, Queen's University Belfast, Stranmillis Road, Belfast, BT9 5AH, United Kingdom. E-mail: b.chen@qub.ac.uk
[b] Department of Materials Science and Engineering, University of Sheffield, Mappin Street, Sheffield, S1 3JD, United Kingdom

† Electronic Supplementary Information (ESI) available: FTIR spectrum of PGS pre-polymer, the measured maximum ethanol uptake and weight loss after the sol extraction of PGSG specimens, FTIR spectrum of gelatin, photographs of PGSG copolymers before and after swelling, the swelling ratio of PGSGs fit to Ritger-Peppas equation, SEM images showing the surface of PGSG specimens after degradation, and *proof-of-concept* fabrication of PGSG20 tissue scaffolds. See DOI: 10.1039/x0xx00000x

View Article Online
DOI: 10.1039/C8PY00544C

angles ranging between 77.5–85.7°.[32–34] As hydration property is an important factor to achieve the optimal biocompatibility, biodegradability, mechanical behaviour, and water-based diffusion characteristics *in vivo*,[32,35] hydrophilic segments such as citric acid and poly(ethylene glycol) (PEG) were incorporated to tackle the hydrophobicity in PGS and develop hydrophilic, water-swellable PGS-based copolymers.[9,32,36–38] Nevertheless, most of these studies focused on the modification of hydration properties of PGS. Only two reported thermo-responsive PGS-based hydrogels owing to the use of PEG,[9,38] and other types of biological stimulus have not been explored. Moreover, the resultant copolymers did not show full biodegradation, which may limit their wider application in biomedical fields.

Gelatin, a natural hydrophilic polymer derived by collagen hydrolysis, is biocompatible, non-immunogenic, non-antigenic, and biodegradable,[39] and its use in medical applications has been approved by U.S. Food and Drug Administration.[40] Furthermore, gelatin contains arginine-glycine-aspartic acid peptide sequence inherited from its parental collagen that promotes cell adhesion and migration.[41,42] Gelatin hydrogels have been applied in many biomedical applications such as cell signalling,[43] gene and drug delivery,[40] tissue engineering,[44] and bio-sensing.[45] Another virtue of using gelatin to design biomaterials comes from its abundant chemical functional moieties such as amine, carboxyl, and hydroxyl groups, which can incorporate further chemical modification, induce hydrophilicity, as well as accept or donate protons in response to the surrounding pH changes.[39,46]

Herein, we design a novel elastomeric, pH-responsive, and fully biodegradable and biocompatible hydrogel system based on copolymers of PGS and gelatin. We hypothesised that this new hydrogel system would have synergistic benefits from (1) networked molecular structure and elastomeric properties of PGS, (2) hydrophilic and pH-responsive properties of gelatin, and (3) a tunable and full biodegradability as well as good biocompatibility from both biopolymers. To avoid the biocompatibility issues with chemical crosslinking agents, the synthesis was performed in a toxin-free manner without any additional crosslinking agents, but by utilising the chemical functional groups from both biopolymers to form ester and amide linkages which directly crosslinked PGS pre-polymer and gelatin. The chemical structure and mechanical behaviour, as well as surface and bulk hydration properties of these new copolymers were investigated using infrared spectroscopy and tensile tests, as well as water contact angle and swelling ratio measurements. The biodegradation kinetics was studied *in vitro* with lipase and collagenase enzymes. Cytotoxicity was examined by cell metabolic assay *in vitro* with L929 mouse fibroblast cells. The potential biomedical applications in controlled drug delivery and soft tissue engineering were demonstrated by pH-responsive drug release tests and *proof-of-concept* fabrication of a 3D, elastomeric and interconnected porous scaffold.

2 Materials and methods

2.1 Materials

Gelatin (Type A, from porcine skin, 300 bloom), sebacic acid, glycerol, ethanol, glycine, hydrochloric acid, phosphate buffered saline (PBS) tablets, Dulbecco's Modified Eagle's Medium (DMEM) with high glucose, resazurin sodium salt, lipase from porcine pancreas (54 U mg^{-1}) were purchased from Sigma-Aldrich. Collagenase (290 U mg^{-1}) was from Thermo Fisher Scientific. Doxycycline hyclate (DOX) and sodium hydroxide was obtained from Alfa Aesar. Gelatin was dehydrated in a vacuum oven at 25 °C for 24 h before use. Water used in this study was prepared by double distillation.

2.2 Preparation of PGS-gelatin (PGSG) copolymers

Copolymerisation of PGS pre-polymer and gelatin was performed in the following procedure: 1) polycondensation of sebacic acid and glycerol to yield PGS pre-polymer; 2) preparation of PGS pre-polymer/gelatin solutions in different weight ratios; 3) synthesis of PGSG pre-polymers; and 4) casting and crosslinking of PGSG pre-polymers into fully cured copolymer films. First, an equimolar mixture of glycerol and sebacic acid was loaded in a three-necked flask, equipped with an oil bath, magnetic stirrer, Dean-stark apparatus, and nitrogen gas line with a bubbler. The monomers were mixed for 30 min, followed by polycondensation at 140 °C for 3 h to produce PGS pre-polymer. In the second step, a specific amount of gelatin (0–20 wt.%) was weighed, and solubilised into the molten PGS pre-polymer by mechanical stirring until transparent and homogeneous solutions were obtained. The yellow to orange coloured low-viscosity PGS pre-polymer/gelatin solutions were then reacted for 24 h at 120 °C to yield viscous resins. The resulting PGSG pre-polymer resins were evenly distributed onto PTFE substrates. After the degassing process in a vacuum oven at 80 °C for 1 h to remove the air bubbles, crosslinking was continued further for 24 h at 120 °C to achieve fully cured copolymer films. Finally, all the samples were washed four times using 0%, 30%, 70%, and 100% water-ethanol solutions for 12 h each at 40 °C. The un-crosslinked proportion of cured copolymers was determined by the weight difference on a 4-decimal scale (Sartorius M-power, Germany) before and after the washing steps. The solubility of PGSG pre-polymer and cured copolymer samples was evaluated by immersing the samples in various solvents, namely, 1,4-dioxane, acetone, chloroform, dimethylformamide, ethanol, tetrahydrofuran, and water, for 48 h at 37 °C. The nomenclature of the prepared PGSG copolymers is presented as PGSGX, where "X" stands for the weight percentage of gelatin in PGSG copolymers: PGSG0, PGSG5, PGSG10, PGSG15, and PGSG20.

2.3 Characterisation of PGSGs

The number average molecular weight ($\bar{M}_n$), weight average molecular weight ($\bar{M}_w$) and polydispersity index (PDI) of PGS pre-polymer before copolymerization with gelatin were measured by gel permeation chromatography (GPC, Agilent

View Article Online
DOI: 10.1039/C8PY00544C

1260 GPC System), with tetrahydrofuran as the mobile phase and polystyrene standards for calibration.

Attenuated total reflectance Fourier transform infrared (FTIR) spectroscopy was conducted on a Perkin Elmer Spectrum One NTS analyser (500–4000 cm^{-1}, Resolution: 2 cm^{-1}, number of scans: 16). A pressure of 70 N was applied using a built-in screw to increase the extent of sample contact with the diamond ATR crystal.

The microscopic surface analysis was carried out by scanning electron microscopy (SEM) (Philips XL 30S FEG; spot size = 3, accelerating voltage = 10 kV). The samples were cut into small pieces and attached onto an aluminium stub by applying a Pelco® conductive silver paste (Ted Pella, USA). A gold-coating was applied using a high resolution polaron sputter coater (Emscope SC500A) to reduce the charge-up effects.

Mechanical property of dry and hydrated PGSG samples was determined by tensile tests using a Hounsfield H100KS (Tinius Olsen), according to the ISO 527. The specimens were punched-out into dog-bone shapes (n = 6, thickness: 0.32–0.46 mm) using a mould stencil (Ray-ran Test Equipment). A 10 N load cell was used at the strain rate of 50 mm min^{-1}. For the testing of hydrogels, the specimens were swollen in PBS solution at 37 °C for 72 h, and tested under the same tensile condition as above. The test results are reported in a manner of mean ± standard deviation.

The crosslink densities of cured PGSGs were determined by Eq. (1), based on the theory of rubber elasticity.

$$n = \frac{E}{3RT} \#(1)$$

where n is the density of active network chains, E is the Young's modulus, R is the universal gas constant, and T is the temperature during the tensile test.[47]

The surface and bulk hydration properties of PGSG specimens were determined by water contact angle and swelling studies. The water contact angle on the PGSG samples was measured using a drop shape analyser (DSA-100, Krüss, Germany). A droplet of water (10 µL) was dosed onto the sample surface using a 22-gauge, blunt-end syringe needle. The angle measurement was done by capturing high-resolution images after 10 seconds. The bulk hydration properties were analysed by swelling behaviour of PGSG specimens in PBS. Dry PGSG specimens (n = 5; diameter: 5.3 mm; thickness: 0.41 ± 0.09 mm) with known initial weight (W_{dry}) were prepared by a hydraulic press and disc-shaped mould stencil. The specimens were fully immersed in the medium and incubated at a physiological temperature of 37 °C. At specific time intervals, the swollen specimens were collected, blotted with a filter paper to remove the excessive surface water, and weighed (W_{wet}). The swelling ratio was determined by Eq. (2).

$$Swelling\ ratio\ (\%) = \frac{W_{wet} - W_{dry}}{W_{dry}} \times 100 \#(2)$$

2.4 pH-responsive swelling and drug release tests

The pH-responsive swelling ratio of PGSGs was measured using the following two buffer solutions: citrate buffer (pH 5.0), and glycine-NaOH buffer (pH 9.1), at 37 °C, and calculated using Eq. (2). The pH-dependent drug release profiles of the PGSG20 were evaluated. DOX was selected as a model drug, as it is one of the most commonly prescribed antibiotics for soft tissue infections.[48] The drug loaded PGSG20 specimens (n = 5; diameter: 5.3 mm; thickness 0.40 ± 0.11 mm) were prepared by soaking in 10 mL of DOX water solution (pH 6.2, 10 mg mL^{-1}) for 72 h at 4 °C to minimise drug denaturation, followed by washing twice with fresh water to remove the excessive surface-adsorbed drug and drying in a vacuum oven at 37 °C for 48 h. The specimens were then immersed in 10 mL of citrate buffer, PBS, and glycine-NaOH buffer solutions for the release tests. The buffer solutions were used here again not only to modulate the pH values of drug releasing media, but also to minimise the non-specific Coulomb interactions between DOX and PGSG.[49] At scheduled time intervals, 1 mL of the medium was collected and replaced by a fresh medium. The cumulative drug release profiles were obtained by measuring the absorbance of collected media at 345 nm (λ_{max}) and pre-prepared calibration curve of known drug concentrations using an ultraviolet-visible spectrophotometer (UV-vis, Perkin Elmer Lambda 900, US).[50] The drug loading capacity of PGSG20 hydrogels was measured as 0.41 ± 0.05 mg per specimen (*i.e.*, 3.8 ± 0.6 wt.% of the dried specimen) by the same spectroscopic analysis as above using the drug loading solutions before and after the loading procedure.

2.5 Biodegradability and cytotoxicity tests *in vitro*

The degradation behaviour of the PGSG hydrogels was investigated *in vitro*. The specimens (n = 5; diameter: 5.3 mm; thickness: 0.43 ± 0.15 mm) were sterilised in 70% ethanol and dried in a vacuum condition until constant weights were observed. The incubation was carried out in the following degradation media: 1) PBS without enzymes, 2) PBS with lipase (110 U L^{-1}), and 3) PBS with collagenase (62 U L^{-1}). The concentration of enzymes in this test was decided based on the serum activity of enzymes in healthy adults found in previous literature.[51,52] The media were kept fresh by replacement daily to ensure the full enzyme activity. The incubation was performed at 37 °C in a shaker incubator at 100 rpm (Stuart SI500). After 3, 7, 14, 21, and 28 days, the weight loss by degradation was determined after washing the specimens with a copious amount of water to remove surface bound enzymes and drying in vacuum. The percentage weight loss was calculated by the following Eq. (3), where W_{ini} and W_{day} are the initial weight (215 ± 17 mg) before degradation and the weight measured at the specific incubation day, respectively.

$$Weight\ loss\ (\%) = \frac{W_{ini} - W_{day}}{W_{ini}} \times 100 \#(3)$$

Cytotoxicity of PGSGs was analysed by cell metabolic assay using resazurin *in vitro*. Prior to the cell seeding, all the

View Article Online
DOI: 10.1039/C8PY00544C
ARTICLE Journal Name

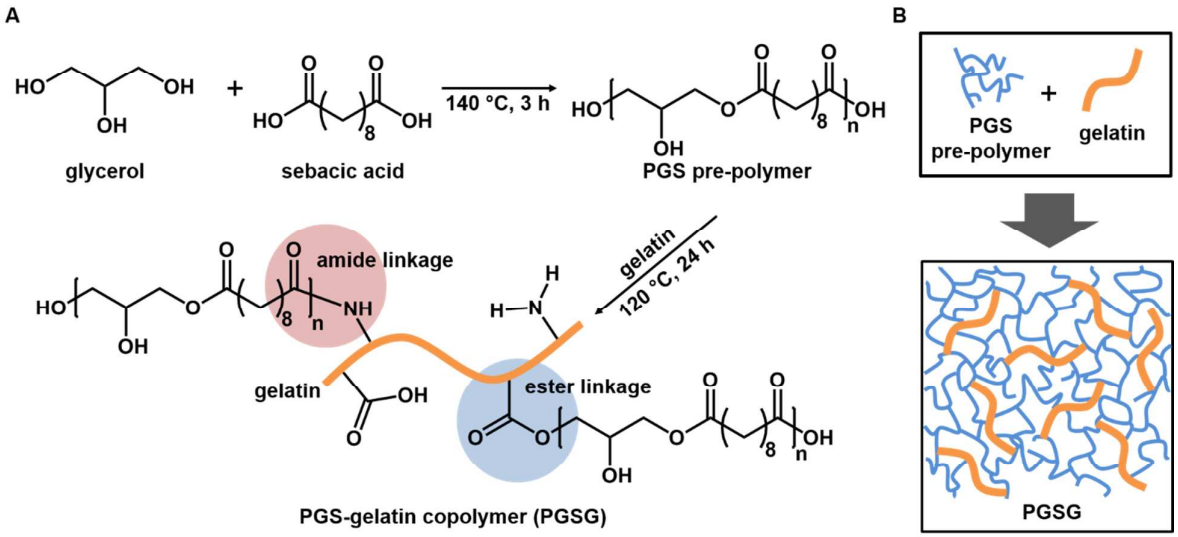

Fig. 1 (A) Synthetic scheme of PGSG copolymers. (B) Sketch showing the formation of the macromolecular network consisted of directly crosslinked PGS pre-polymer and gelatin.

specimens were sterilised by 70% ethanol, washed thrice with plenty of water and soaked in DMEM overnight in an incubator (37 °C, 5% CO_2). PGSG specimens were then placed in a 12-well plate and fixed by metal rings for cell seeding. After cell trypsinisation with trypsin-ethylenediaminetetraacetic acid, trypsin activity was neutralised with 5 mL of warm medium, and the cells were collected by centrifugation (1000 rpm, 5 min). The optimum cell density (3.0×10^4 cells per specimen) was obtained by dilution with DMEM and seeded onto PGSG specimens. Cell-free and cell-only tests were also performed for negative/positive control, and used to normalise the data. After 3 days of incubation, the DMEM was removed from the well plate and the cell-seeded specimens were washed with PBS and placed in a new well plate. One mL of resazurin solutions (0.1 mM in PBS) was added to each sample and incubated for 2 h. The absorbance at 570 nm was recorded using a colorimetric plate reader (Bio-TEK). This assay was repeated on day 6, 9, 12, and 15. Microscopic images were taken by an optical microscope (Motic, AE2000 Inverted Microscope) to observe cell morphology on the specimen surfaces. The experiments were triplicated and the data was reported as mean ± standard deviation.

2.6 Statistics

All measurements were reported as mean ± standard deviation with a confidence level of 95% unless otherwise stated. Two-way analysis of variance (ANOVA) was used to determine the differences in the *in vitro* cell metabolic assay results in respect to the test time and material. A p value < 0.05 was considered to be statistically significant.

3. Results and discussion

3.1 Synthesis and characterisation of PGSG hydrogels

PGSG copolymers with varying ratio between PGS pre-polymer and gelatin were synthesised by a thermal crosslinking approach (Fig. 1A and B). The first step involved polycondensation of glycerol and sebacic acid to produce PGS pre-polymer. The synthesis of PGS pre-polymer was confirmed by FTIR with the distinct peaks at 1176 cm^{-1} and 1733 cm^{-1}, which is attributed to the formation of ester linkages between hydroxyl groups from glycerol and carboxyl groups from sebacic acid (Fig. S1).[47,53,54] However, the absorption bands of hydroxyl and carboxyl groups are still shown in the spectrum of PGS pre-polymer. This indicates that the PGS pre-polymer is not fully cured, therefore further chemical crosslinking is possible with the functional groups. GPC analysis affirmed the synthesis of PGS pre-polymer with the $\bar{M}_n$, $\bar{M}_w$, and PDI values of 455, 1875, and 4.12, respectively. It should be noted that

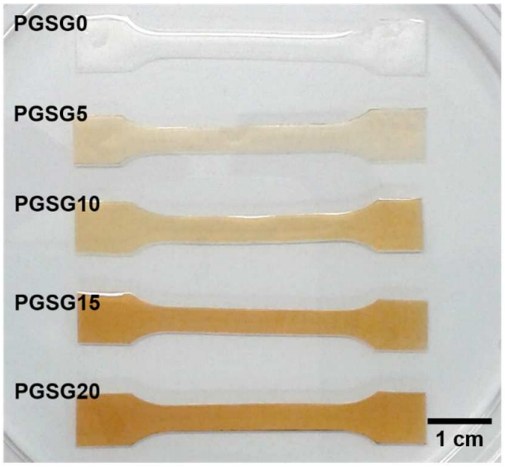

Fig. 2 A photograph showing fully-cured PGSG copolymer specimens with various gelatin contents. The colour change from pale yellow to orange was observed due to the addition of gelatin in copolymer synthesis.

View Article Online
DOI: 10.1039/C8PY00544C

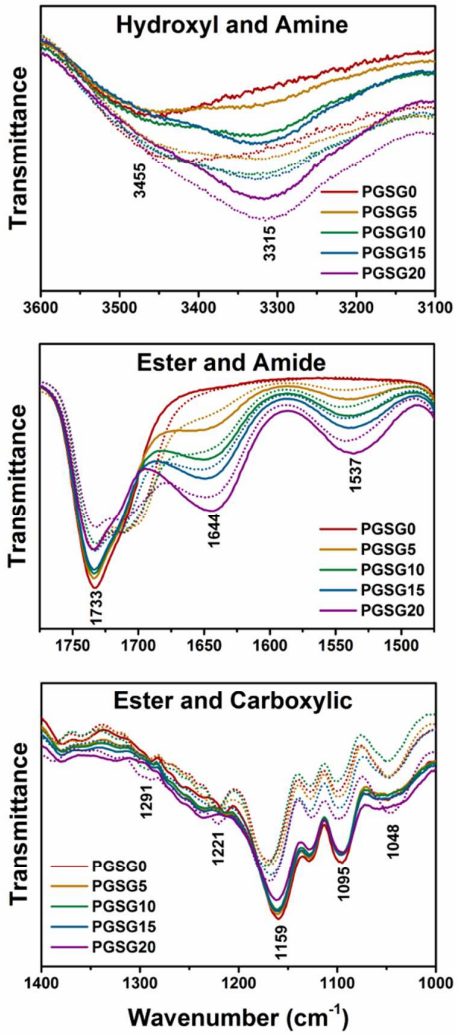

Fig. 3 ATR-FTIR spectra of PGSG copolymers before and after crosslinking. The dotted lines and solid lines refer to the PGSG pre-polymers and cured copolymers, respectively.

the PGS pre-polymer in this study was synthesised by a relatively short reaction time to achieve low molecular weight, which facilitates further copolymerisation with gelatin. In the second step, gelatin was added to and reacted with PGS pre-polymer to yield PGSG pre-polymers. The PGSG pre-polymers were then further crosslinked thermally to produce fully cured PGSG copolymer films. The prepared PGSG copolymers are characterised by soft mechanical properties and the gloss surfaces with the distinct yellow to orange colours depending on the concentration of gelatin as seen in Fig. 2.

The PGSG pre-polymers before curing were found to be soluble in 70% ethanol-water solution. Moreover, the pre-polymers were re-meltable and deformable into a desired physical morphology, enabling fabrication of complex architectures such as an interconnected porous scaffold for tissue engineering applications (discussed below). The un-crosslinked proportion (sol) of cured PGSG copolymers was determined by the weight loss after extraction with a series of warm water-ethanol solutions and showed a minimal increase from 16.4 to 19.4% with the addition of gelatin (Fig. S2).

All the cured and purified PGSGs were not dissolved, but rather swelled in 1,4-dioxane, acetone, chloroform, dimethylformamide, ethanol, tetrahydrofuran, and water. The maximum uptake of ethanol of PGSG specimens after 48 h of immersion at 37 °C was measured as 58.0–69.5% (Fig. S2), inversely proportional to the amount of gelatin within copolymers. This amphiphilic swelling characteristics in PGSG copolymers, driven by copolymers of hydrophobic PGS and hydrophilic gelatin, suggests that post-functionalisation with desired chemical species is possible, such as the loading of a drug into the hydrogel by diffusion (discussed below).

As we previously discussed, the PGS pre-polymer consisted of a network macromolecular structure with the hydroxyl and carboxyl groups from its monomers, glycerol and sebacic acid (Fig. S1). Gelatin is a protein, therefore it contains amide backbone structure with amine and carboxyl groups from its amino acid sequence (Fig. S3). During the thermal curing process of PGS pre-polymer and gelatin by polycondensation reactions, the hydroxyl and carboxyl groups would yield ester bonds, whereas amide bonds would be formed between amine and carboxyl groups (Fig. 1).[55] The proposed chemical structure of PGSG copolymers was affirmed under FTIR by comparing PGSG pre-polymers and cured copolymers, as shown in Fig. 3.

The ester bonds in PGSG pre-polymers were confirmed by intense peaks at 1733 cm^{-1} (C=O) as well as 1159 cm^{-1} and 1095 cm^{-1} (C-O). After the thermal curing of PGSG pre-polymers into copolymers, the intensity of the ester bond peaks was further enhanced, indicating the newly formed ester bonds between the polymer chains.[47,53] On the other hand, the intensities of hydroxyl peak at 3455 cm^{-1} (O-H) and carboxyl peaks at 1291 cm^{-1}, 1221 cm^{-1} and 1048 cm^{-1} (C-O) were reduced due to the curing process.[47,53] Regarding the amide bond, the peak intensities of amide I at 1644 cm^{-1} (C=O) and amide II at 1537 cm^{-1} (N-H and C-H) in PGSG pre-polymers were also further enhanced in the cured copolymers,[56] whereas the peak intensities of amine at 3315 cm^{-1} (N-H) and carboxyl (also partially due to the ester bonds) were reduced by forming the new amide bonds.

When the cured PGSG copolymers were compared between each other, it was found that with an increasing gelatin content the amide peaks (at 1644 cm^{-1} and 1537 cm^{-1}) became stronger while the ester bond peaks (at 1733 cm^{-1}, 1159 cm^{-1}, and 1095 cm^{-1}) diminished gradually. These results are attributable to two factors: (1) gelatin has amide groups in its backbone, leading to an increase in the amide content in the copolymer with a higher gelatin content; and (2) the amine groups in gelatin react with hydroxyl groups competitively against carboxyl acid groups as previously described, resulting in more amide bonds and fewer ester bonds in the copolymer.

Hydration properties of cured PGSG copolymers were investigated in both surface and bulk characteristics. First, the surface hydration property was analysed by measuring the water contact angles (Fig. 4A). In this test, a droplet of water

View Article Online
DOI: 10.1039/C8PY00544C

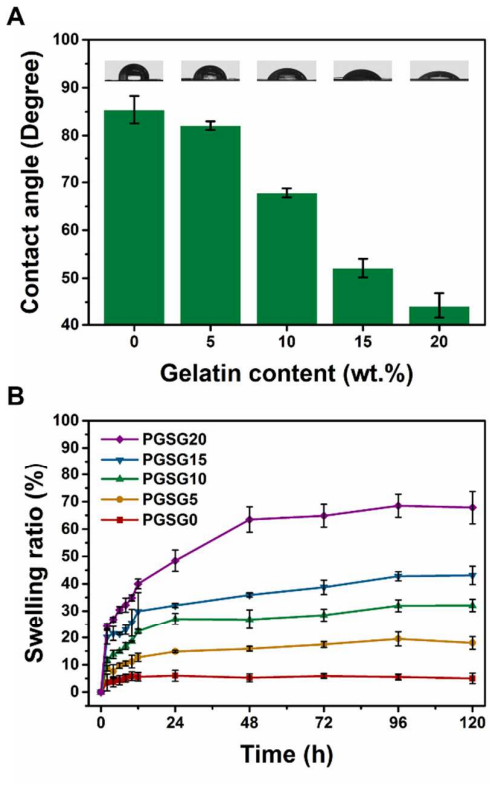

Fig. 4 (A) The surface water contact angle of PGSG copolymers. The inset photographs show the shape of water droplets on the surface of PGSG specimens. (B) Percentage swelling ratio of PGSG copolymers (PBS, 37 °C) from 0 to 120 h. The incorporation of gelatin within PGS greatly improved the water uptake by a maximum 13-fold increase.

was dosed on the sample, and the angle between the sample surface and the tangent line to the water drop was measured. A higher contact angle implies lower surface wettability and higher hydrophobic surface characteristics. PGSG0 exhibited a high water contact angle of 85.4 ± 2.9°, similar to the previous report for pristine PGS.[33] Incorporation of hydrophilic gelatin in PGSGs greatly improved the surface wettability with decreases in water contact angle. The lowest water contact angle of 44.2 ± 2.7° was measured from PGSG20, which is generally considered as a hydrophilic surface.[34] This improvement of surface wettability makes the PGSG copolymers more attractive for tissue engineering applications, as cells are known to adhere to and proliferate on hydrophilic surfaces better than on hydrophobic surfaces.[35] The surface hydrophilicity is also an important parameter in wound dressing applications. The better surface wettability, the higher adsorption of the exudates in the wound sites, promoting healing process.[57,58]

Secondly, the bulk hydration properties of PGSG copolymers were determined by measuring their water swelling ratio. In this test, PGSG copolymers were immersed in PBS at 37 °C, and the amounts of water uptake were recorded in specific time intervals. Fig. 4B shows the swelling ratio of PGSG up to 120 h. All the PGSG specimens showed the equilibrium water uptake after 72 h of immersion and volume expansion by swollen water (Fig. S4). While PGSG0 exhibited a minimal water swelling ratio of 5.0 ± 1.9%, incorporation of 20 wt.% gelatin in PGSG20 induced almost a 13-fold increase in water uptake of 67.8 ± 5.9%, resulting in swollen hydrogels.

The kinetics in water diffusion into the PGSG polymer matrix was further investigated mathematically in order to understand the determining mechanisms of swelling process. The data points at the early stage (W_t/W_{eq} < 0.6) were fit to the following Ritger-Peppas equation, Eq. (4),

$$\frac{W_t}{W_{eq}} = kt^n \#(4)$$

where W_t and W_{eq} are the water uptake values at a specific time (t) and at equilibrium, respectively.[5,59] k is the characteristic swelling constant and n is the determining factor of the mode of water transport through the copolymers. The calculated n values for PGSG5, PGSG10, PGSG15, and PGSG20 were 0.28, 0.33, 0.37, and 0.49 respectively (Fig. S5) (PGSG0 was omitted here due to the minimal water swelling ratio), indicating Fickian diffusion. In this diffusion process, the water penetration rate in the gels is slower than the polymer chain relaxation rate.[60] In other words, the elastic polymer chains in PGSG copolymers instantaneously responded to the stress given by water absorption, thereby the water diffusion through the polymer matrix is not limited by the relaxation of polymer networks. Fickian diffusion is known to be an asset in building diffusion-controlled drug delivery systems from an aqueous stimulus.[32,61,62]

3.2 Elastomeric mechanical properties

The mechanical properties of dry and hydrated PGSG copolymers were evaluated by uniaxial tensile tests and the results are shown in Fig. 5. In respect of the tensile properties of dry specimens, PGSG0 featured Young's modulus, tensile strength, and strain to failure of 0.59 ± 0.05 MPa, 0.55 ± 0.07 MPa, and 142 ± 17%, which are in agreement with PGS homopolymers in previous reports.[12,47] The effect of gelatin on the tensile modulus and strength of PGSGs was measured by an almost 9-fold increase in modulus and 14-fold increase in strength from PGSG0 to PGSG20. The crosslinking densities calculated by Eq. (1) were 80.2 (PGSG0), 114.1 (PGSG5), 127.7 (PGSG10), 249.9 (PGSG15), and 812.3 mol m^{-3} (PGSG20), respectively, showing an increase in the crosslinking density with increasing gelatin content. When even higher gelatin contents (30 and 40 wt.%) were used, the resultant copolymers were extremely brittle and could not be stretched or bended (hence not tested in this study), confirming that the crosslinking density is increased by the addition of a higher amount of gelatin. The increased crosslinking densities in PGSGs are accounted for by the additional ester and amide linkages provided by the crosslinking between PGS pre-polymer and gelatin, which was confirmed by FTIR previously.

The changes in tensile properties of PGSG copolymers can also be attributed to the mechanical properties of gelatin. As gelatin has relatively high tensile modulus and strength of 3.0

View Article Online
DOI: 10.1039/C8PY00544C

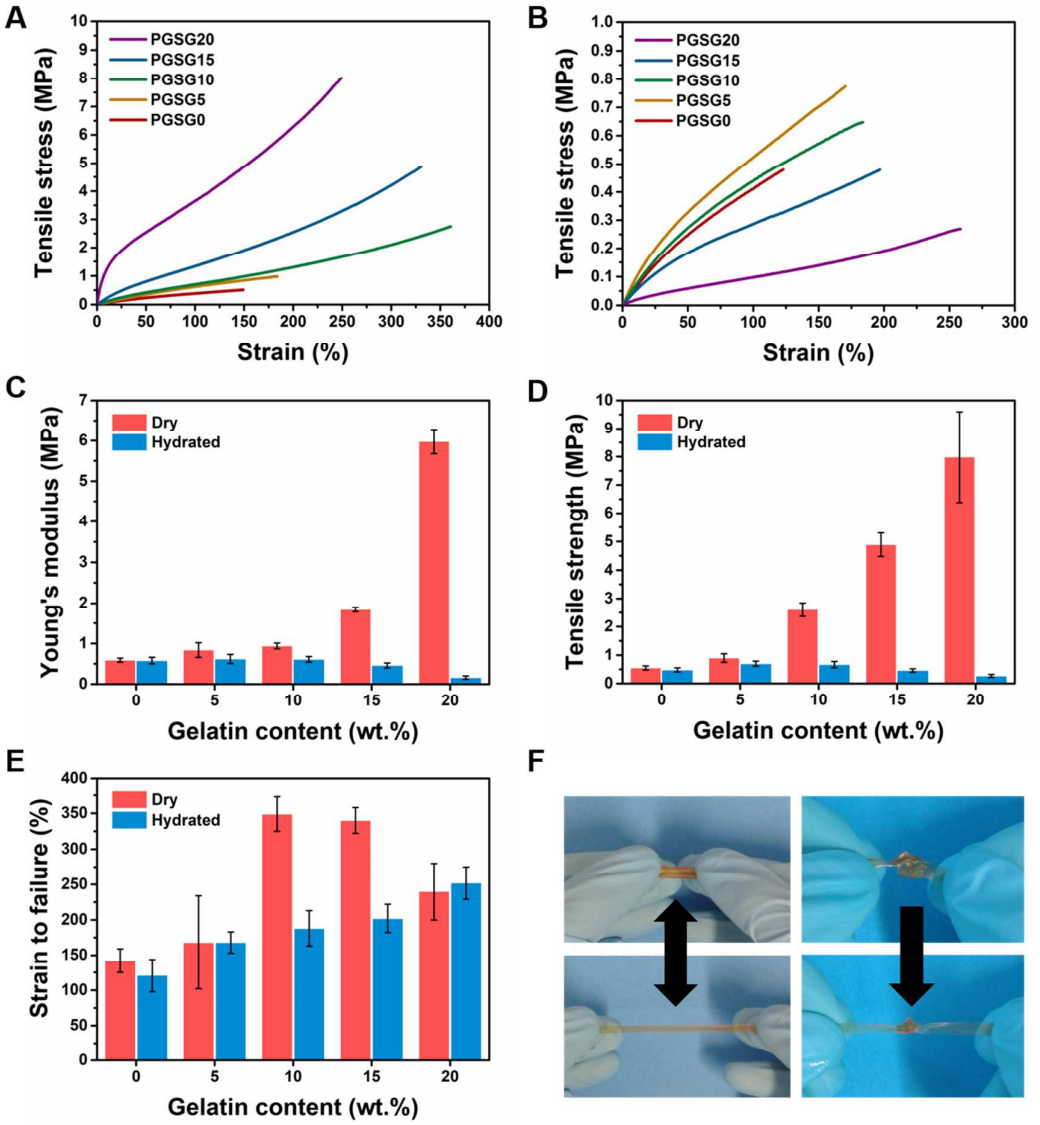

Fig. 5 Tensile properties of PGSG copolymers. The representative tensile stress-strain curves of (A) dry, and (B) hydrated PGSG copolymers. (C) Young's modulus, (D) tensile strength, and (E) strain to failure values of PGSG copolymers, both dry and hydrated. (F) Demonstration of mechanical stretching and knotting with hydrated PGSG20 specimens.

GPa[63] and 63.2 MPa,[64] the addition of gelatin to PGS gives PGSG copolymers with higher stiffness and strength compared to the PGS homopolymer. The amide bond is, in general, known to be more rigid than the ester bond due to the partial double bond character through tautomerism.[65,66] According to the FTIR analysis earlier, the PGSGs with a higher content of gelatin have more amide bonds than those with a lower content of gelatin, thereby showing a higher stiffness.

Interestingly, the strain to failure of dry PGSG specimens also shows an increase between PGSG0 (PGS homopolymer) and PGSG15 copolymers. Although the addition of gelatin increased the crosslinking density in PGSG as calculated above, gelatin has highly coiled molecular structures, therefore one can expect that the relaxation of gelatin coils promoted higher ductility in PGSG.[63,64,67] However, too high crosslinking density in PGSG20 became a dominant factor which drastically decreased free volume in the polymer matrix and restricts the molecular motion, resulting in a decrease in strain to failure.[68]

PGSGs featured highly elastomeric mechanical behaviours even in fully swollen state. Complex deformations such as stretching and knotting were possible with hydrated PGSGs, as demonstrated in Fig. 5F. With the increasing gelatin amount in hydrated PGSGs, the Young's modulus and tensile strength were decreased from 0.62 ± 0.08 MPa to 0.16 ± 0.04 MPa and from 0.70 ± 0.07 MPa to 0.27 ± 0.05 MPa. In contrast, the strain to failure value increased from 121 ± 23% to 252 ± 23%, primarily due to the higher polymer chain flexibility led by higher water swelling ratio as discussed previously.

View Article Online
DOI: 10.1039/C8PY00544C

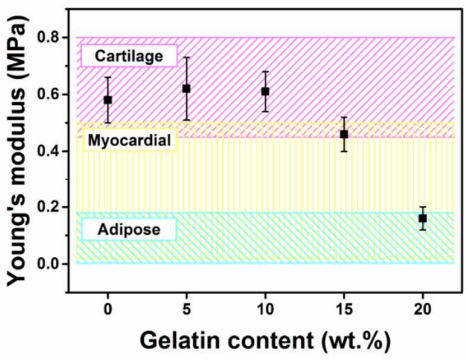

Fig. 6 Comparison of Young's modulus of PGSG hydrogels to that of native tissues from the literature. Each shaded area represents the range of Young's modulus of cartilage[69] (magenta), myocardial[16] (yellow), and adipose[13] (cyan) tissues.

As shown in Fig. 6, the tensile modulus values of hydrated PGSG copolymers are in the range of soft tissues such as adipose, myocardial, or cartilage tissues,[13,16,69] illustrating a promising future of PGSGs in soft tissue engineering. With their biomimetic mechanical behaviours, porous tissue scaffolds were fabricated with PGSG20 as a *proof-of-concept* (Fig. 7). The PGSG pre-polymers were re-meltable and easily deformable into a desired shape, therefore fabrication of a three-dimensional and large scaffold was feasible by a combined technique of salt-leaching and freeze-drying (see SI for the detailed fabrication technique). The macro-pores were generated by salt crystals (300 µm) in the salt-leaching stage, whereas the micro-pores were formed by the ice crystals during freeze-drying. The benefits of well-defined and interconnected pore structures as well as the micro-pores shown in Fig. 7B and C are well-demonstrated in tissue engineering fields, with the ability to help cell penetration and proliferation, as well as transportation of chemical species such as water, gas, nutrients, and metabolic waste products throughout the tissue scaffolds.[70,71] The prepared scaffold is also highly elastomeric and exhibits excellent shape recovery after the release of a compressive load, with compressive Young's modulus and compressive stress at 75% strain of 0.19 ± 0.05 MPa and 1.16 ± 0.40 MPa, respectively (Fig. 7D and E). The interconnected pore structures and elastomeric mechanical properties, as well as good biocompatibility and controllable biodegradation (discussed below) make this PGSG scaffold an attractive candidate for applications in soft tissue engineering. Future work may include dynamic and cyclic mechanical tests with PGSG porous scaffolds under simulated body conditions to fully illustrate the advantages associated with the elastomeric properties of PGSGs and explore them further as potential candidates in soft tissue engineering.

3.3 pH-responsive behaviours

In our body, there is a large variation in pH in terms of the physiological roles and medical conditions. For instance, the gastric pH is highly acidic ranging between 1.0 and 2.5 (up to 5 when fed), whereas the proximal small intestine exhibits almost neutral pH of 6.6.[72,73] The healthy skin surface has slightly acidic pH of 5.5, however the injured skin tissue in burn patients features basic pH values ranging between 9.5–10.5.[74]

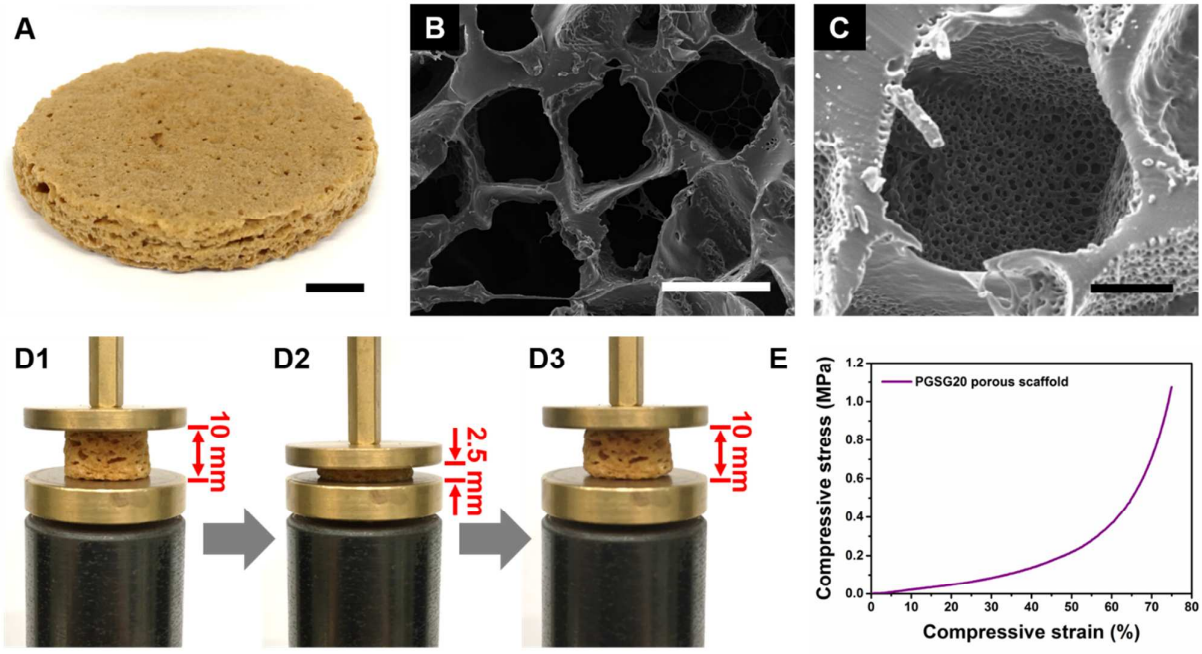

Fig. 7 (A) Photograph showing a *proof-of-concept* tissue scaffold fabricated from PGSG20 (scale bar: 1 cm). (B) Well-defined and interconnected porous microstructures seen in an SEM image (scale bar: 300 µm). (C) A closer look at a pore revealing micro-pores on the wall surface (scale bar: 100 µm). (D1 – D3) Elastomeric PGSG20 porous scaffold showing excellent shape recovery after the release of a compressive load. (E) A representative compressive stress-strain curve of PGSG20 scaffold.

View Article Online
DOI: 10.1039/C8PY00544C

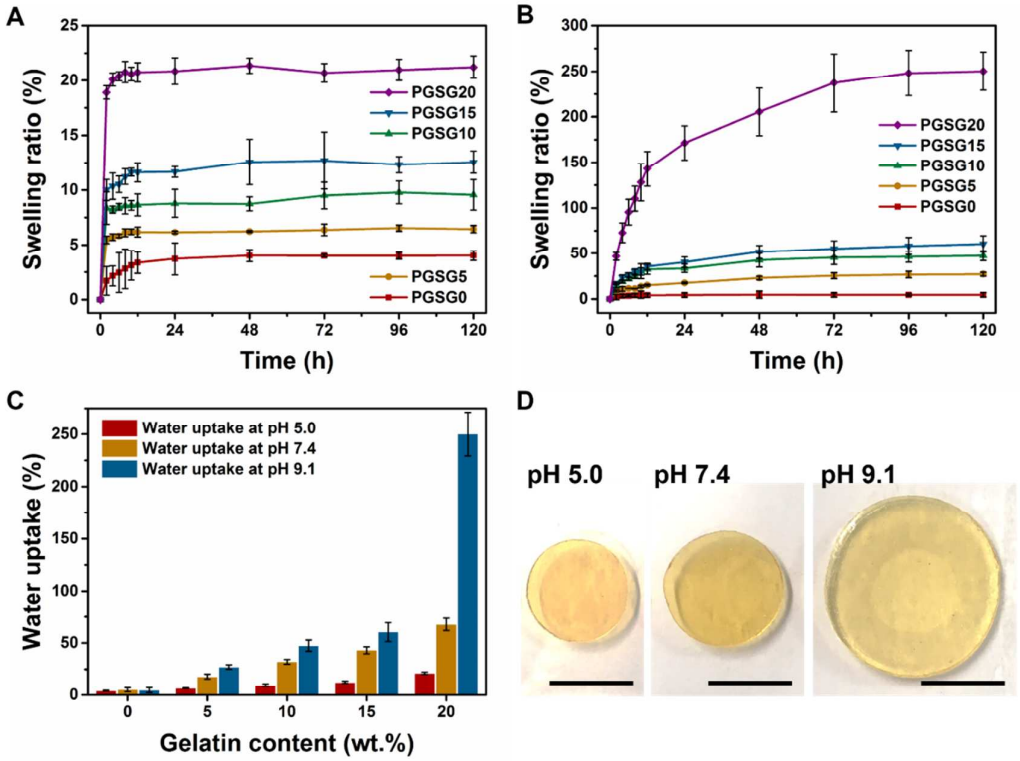

Fig. 8 pH-responsive water swelling ratio of PGSGs measured at (A) pH 5.0 and (B) pH 9.1. (C) The equilibrium water uptake of PGSGs in three different pHs (the equilibrium water uptake at pH 7.4 was derived from Fig. 4. (D) Pictures of PGSG20 specimens after 72 h of hydration at pH 5.0, 7.4, and 9.1 (scale bars: 5 mm).

Hydrogels with pH-responsive properties, therefore, are of great interest in many biomedical fields, with their ability to alter the material structure and properties depending on the surrounding biological pH values.

Hydrogels containing ionic groups respond to external pH, making them pH-responsive hydrogels.[75] As shown previously in FTIR study, although some amine and carboxyl groups were sacrificed to form covalent linkages in PGSG, there were still ionic functional groups remained in copolymer hydrogels. Therefore, the pH-responsiveness of PGSG hydrogels was examined by swelling tests in three different pHs. Fig. 8A and B illustrate the water swelling ratio of PGSG specimens in acidic (citrate buffer, pH 5.0) and basic (NaOH-glycine buffer, pH 9.1) pHs. Fig. 8C shows the equilibrium water uptake values of PGSGs in three different pHs (pH 5.0, 7.4, and 9.1). The higher the pH value was the higher the water swelling ratio was achieved in PGSG20. The values of the water uptake at equilibrium measured at pH 5.0 were 4.0 ± 0.5% (PGSG0), 6.4 ± 0.3% (PGSG5), 9.6 ± 1.4% (PGSG10), 12.5 ± 1.0% (PGSG15), and 21.2 ± 1.0% (PGSG20), which indicates the PGSG copolymers swell less in an acidic pH than in a neutral pH condition. In contrast, the swelling ratio of PGSG copolymers at pH 9.1 increased greatly, to the values of 27.1 ± 2.1% (PGSG5), 47.5 ± 5.5% (PGSG10), 60.5 ± 9.0% (PGSG15), and 250.2 ± 21.1% (PGSG20), while it was not changed much in PGSG0 homopolymer (4.6 ± 2.5%). The pH also affects the kinetics in the equilibrium of water swelling for the copolymers. It was shown previously that the equilibrium was acquired in 72 h at pH 7.4. In acidic condition (pH 5.0), 12 h was enough to reach equilibrium at pH 5.0, whereas a longer time of 96 h was required at pH 9.1.

This pH-responsive swelling behaviour found in PGSG copolymers is different to that of neat gelatin. The latter shows the minimum swelling ratio at the isoelectric point near the neutral pH (pH 7–9, type A, form porcine skin), where anionic and cationic forms are exactly balanced resulting in chain collapse.[40,76] In contrast, PGSG copolymers showed the minimum swelling at the acidic pH and the maximum was achieved at the basic pH. It can be concluded that the number of ionisable carboxyl groups is higher than that of amine groups in PGSG copolymers. The carboxyl group (-COOH) ionises by deprotonation, becoming negatively charged carboxyl groups ($-COO^-$). The amine group ($-NH_2$), on the other hand, becomes positively charged groups by accepting protons ($-NH_3^+$). To acquire the electrostatic repulsion that leads to the higher swelling ratio of PGSG copolymers in basic pH conditions as described above, the deprotonation of carboxyl group should be dominant and counter the protonation of amine group.[77] This is attributable to the fact that the amine groups are supplied only by the relatively minor amount of gelatin in the synthesis of PGSG copolymers, whereas the carboxyl group was offered by both PGS pre-polymer and gelatin becoming abundant within PGSG copolymers.

View Article Online
DOI: 10.1039/C8PY00544C
ARTICLE Journal Name

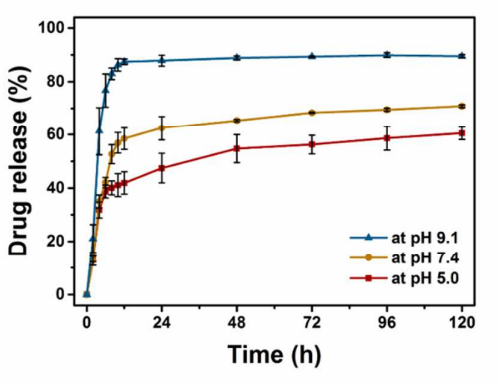

Fig. 9 Cumulative drug release profile of DOX from PGSG20 at three different pH values.

It was also noted that the swelling ratio of PGSG20 at pH 9.1 was much greater than that of other PGSGs. In amphiphilic hydrogels such as PGSGs, the ionisation of functional groups is often hindered by the resistive aggregation of hydrophobic polymer chains.[78] The ionisation of carboxyl groups can happen much more easily in PGSG20 compared to the case with other PGSGs, owing to its much better hydrophilicity arising from the higher gelatin content which provides more chain relaxation and much more free space for the ionisation of carboxyl groups, resulting in a significantly higher swelling ratio of PGSG20 at pH 9.1.

The potential application of pH-responsive PGSGs in controlled drug delivery was investigated selectively on PGSG20 with the greatest pH-responsiveness. PGSG20 specimens loaded with a model drug, DOX, were exposed to the same buffer solutions as for the pH-responsive swelling study (pH 5.0, pH 7.4, and pH 9.1) and the cumulative drug release profiles are depicted in Fig. 9. A quite different drug releasing kinetics was observed from the three different pH values. The drug release kinetics at pH 9.1 quickly reached the equilibrium in 12 h and the cumulative drug release was measured at 89.6 ± 0.6% of the loaded drug amount (or 0.37 mg) initially. However, the cumulative amount of released drug at pH 5.0 was 41.9 ± 4.2% (or 0.17 mg) after 12 h and the equilibrium was not detected even after 120 h. This result suggests a potential use of PGSG copolymers in controlled drug delivery applications. For instance, oral administration of drugs often faces a difficulty in conserving drug stability and drug amount at dynamic gastrointestinal pH conditions.[79] Therefore, pH-responsive PGSG copolymer hydrogels that release drug more slowly and less amount at lower pHs, but more quickly and more amount at higher pHs could be a reliable carrier for controlled drug operations targeting specific organs in the digestive system with pHs ranging from 1 to near 8.[72] The model drug used in this study (DOX) is water-soluble. Since PGSG copolymers exhibit amphiphilic characteristics as discussed previously, future work may also include hydrophobic drugs and steroid hormones to extend their application in controlled drug delivery.

3.4 Biodegradability and biocompatibility *in vitro*

Fig. 10A illustrates the *in vitro* degradation profiles of two selective PGSG samples (PGSG10 and PGSG20) for up to 28 days. Three different degradation media were used in this study; 1) PBS only, 2) PBS + lipase, and 3) PBS + collagenase. Lipase was used to degrade ester linkages, and collagenase was to break down gelatin. Both the PGSG10 and PGSG20 exhibited weight losses of 7.5 ± 3.3% and 8.1 ± 2.1%, respectively after 28 days of incubation in the PBS only medium. In contrast, the presence of enzymes led to accelerated degradation kinetics of PGSG specimens, and lipase appeared to be yielding more polymer degradation than collagenase. This was expected as the majority of PGSG copolymers is PGS (polyester) rather than gelatin. PGSG20 presented faster enzymatic degradation kinetics compared to that of PGSG10, which can be assigned to the better hydration properties of PGSG20 as demonstrated previously in water swelling ratio. PGSG10 yielded a weight loss of 33.2 ± 1.9% with lipase and 15.2 ± 4.6% with collagenase, whereas PGSG20 underwent the weight losses of 69.3 ± 1.0% with lipase and 54.1 ± 2.0% with collagenase after 28 days. It should be noted that the degradation rates of PGSGs are faster than that of PGS homopolymer in our previous study with a similar experimental condition (9.6% in enzyme-free media and 29.1% with lipase, after 31 days), which can be attributable again to the presence of gelatin and the higher hydration properties of

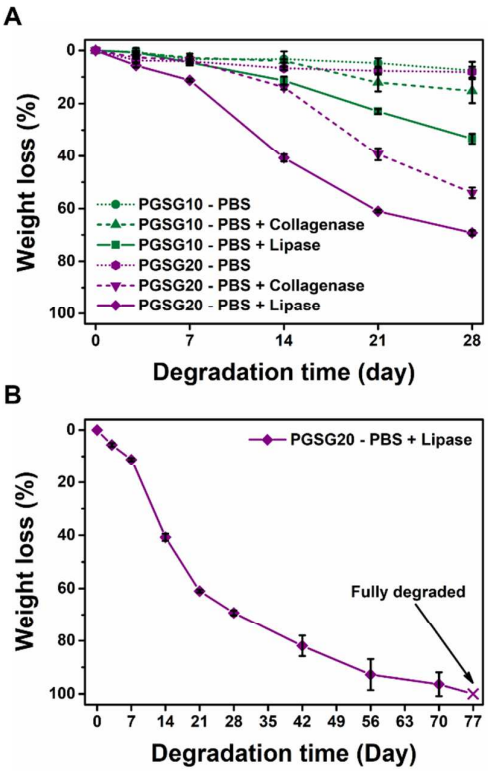

Fig. 10 Percentage weight loss data of (A) PGSG10 and PGSG 20 incubated in PBS solutions with or without the enzymes (collagenase and lipase) for up to 28 days at 37 °C, showing controllable biodegradation, and (B) PGSG20 incubated in PBS solution with lipase enzyme at 37 °C in 77 days showing full degradation.

PGSG copolymers than the PGS homopolymers.[47]

View Article Online
DOI: 10.1039/C8PY00544C

SEM analysis revealed the surface morphology of PGSG specimens after the degradation test with or without enzymes (Fig. S6). The non-enzymatically degraded PGSG specimens featured smooth surfaces in both PGSG10 and PGSG20 due to relatively minor weight losses (less than 10%) as verified previously. However, enzymatically degraded PGSG specimens showed severe surface damages with irregular swelling and pores, indicating the degradation was catalysed by lipase and collagenase enzymes.[47,80] Especially, PGSG20 with lipase enzymes exhibited extremely rough surface morphology with the greatest weight loss found in this study.

In addition, an ultimate full biodegradability was found in PGSG20 in 77 days with lipase (Fig. 10B). Many biomaterials such as tissue scaffolds and drug carriers are not intended to remain permanently in our body.[81,82] For instance, tissue scaffolds should be designed to have the optimal degradation kinetics to match the rate of new tissue formation regenerated by cells and eventually replaced by native tissues.[83,84] In drug delivery systems based on biodegradable polymers, the drug release profile is dependent on the degradation kinetics of polymeric matrix.[81,85] Therefore, the controllable and full biodegradation found in PGSGs is a great asset for their potential uses as biomaterials.

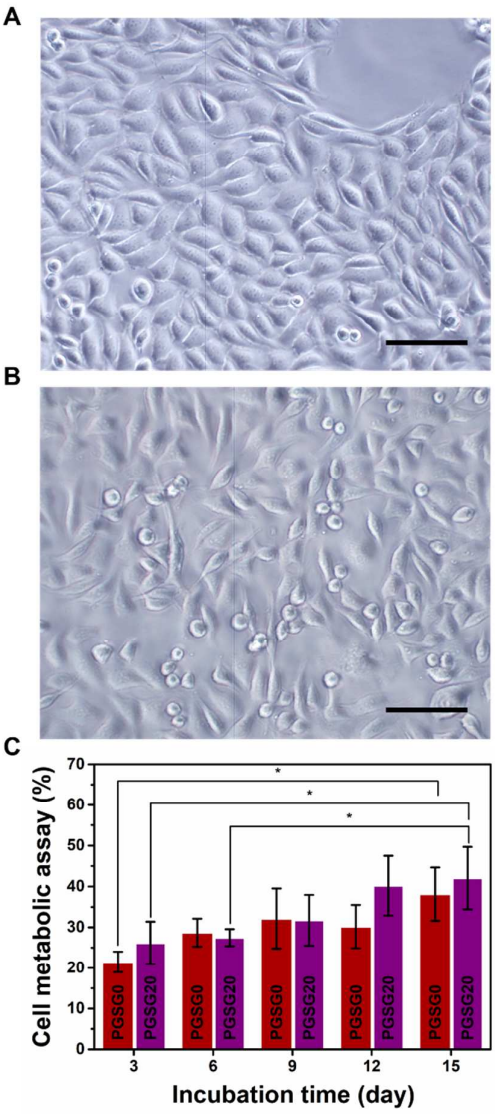

Fig. 11 *In vitro* cell metabolic assay results. (A – B) Optical microscopic images show the cell morphology of L929 fibroblasts cultured on PGSG0 and PGSG20 for 15 days; (A) PGSG0, and (B) PGSG20 (scale bars: 50 μm). (C) The normalised optical density from the resazurin assays of PGS and PGSG20 from 3 to 15 days, demonstrating no cytotoxicity observed from PGSG20 (n = 3; * $p < 0.05$ was considered to be statistically significant).

In vitro cell metabolic assay was conducted on PGSG0 and PGSG20 with resazurin dye and L929 mouse fibroblast cells for up to 15 days. Fig. 11A and B show the morphology of L929 mouse fibroblast cells cultured for 15 days on PGSG0 and PGSG20 specimens. While the cells on both the PGSG0 and PGSG20 appeared to have normal and highly confluent cell populations, PGSG20 showed more adherent, embedded cell morphologies compared to PGSG0. This can be attributed to the better surface wettability of PGSG20, which was demonstrated previously.

No evidence in cytotoxicity was found in the PGSG0 and PGSG20. The cell metabolic activity of both PGSG0 and PGSG20 showed steady growth from day 3 to day 15 (Fig. 11C), with the maximum cell metabolic activity found on day 15 in both cases. The normalised optical density of resazurin dyes increased from 21.5 ± 2.5% to 38.1 ± 6.5% in PGSG0, and from 26.2 ± 5.2% to 42.1 ± 7.6% in PGSG20 from day 3 to day 15. Two-way analysis of variance (ANOVA) was used to determine the statistical significance in respect to the test time and material. Both the PGSG0 and PGSG20 were found to have a significant increase between day 3 and day 15. PGSG20 also presented another significant increase between day 6 and day 15. There was no statistical significance between PGSG0 and PGSG20 in cell metabolic activity, indicating PGSG20 has similar biocompatibility to PGSG0 (PGS homopolymer) *in vitro*. Since PGS has been investigated for various tissue engineering applications due to its well-known good biocompatibility both *in vivo* and *in vitro*,[12,24,25,86] the result suggests that PGSG20 also has great potential in various biomedical fields with its demonstrated biocompatibility in this test. Full assessment on biodegradability and biocompatibility of PGSG hydrogels, which are critical aspects in developing biomaterials for tissue engineering and drug delivery, should be performed with *in vivo* experiments in the future.

4 Conclusions

PGSG copolymer hydrogels with different weight ratios between PGS pre-polymer and gelatin were successfully prepared by condensation copolymerisation followed by swelling in water; the PGS pre-polymer was thermally crosslinked by gelatin during the copolymerisation stage. FTIR studies confirmed that the thermal crosslinking stage induced both ester and amide linkages between the polymers by using the inherent functional groups such as hydroxyl, carboxyl, and amine groups present in both polymers. The improved hydrophilicity of PGSG was determined by the decrease in

View Article Online
DOI: 10.1039/C8PY00544C

water contact angle and the increase in water swelling ratio, resulting in the swollen copolymer hydrogels.

Tensile test results showed that the PGSG copolymer hydrogels had excellent elastomeric properties that endure high and complex mechanical deformations such as stretching and knotting. Their biomimetic mechanical properties were tunable in the range of soft tissues by varying the gelatin content in PGSG copolymers. The potential use of PGSG copolymers in soft tissue engineering was further demonstrated by the possibility of manufacturing a 3D, elastomeric, and interconnected porous scaffold.

The pH-responsive behaviour of PGSG copolymers was analysed by the dramatic differences in water uptake at acidic, neutral and basic pHs due to the ionisable functional groups found under FTIR studies. The potential of PGSG copolymers as a pH-controlled drug delivery system was also validated by pH-responsive drug release tests. The controllable and full biodegradation of PGSG was shown by biodegradation tests *in vitro* with lipase and collagenase enzymes. The biocompatibility of PGSG was confirmed, with no evidence in cytotoxicity by cell metabolic assay as well as highly confluent, well adherent morphology of cultured fibroblast cells.

These results suggest that the multifunctional PGSG copolymer hydrogels created in this study have great prospective in various biomedical fields such as soft tissue engineering and controlled drug delivery.

Conflicts of interest

There are no conflicts to declare.

Acknowledgements

S. Y. thanks the University of Sheffield for a University Prize Scholarship.

References

1 Q. T. Nguyen, Y. Hwang, A. C. Chen, S. Varghese and R. L. Sah, Biomaterials, 2012, 33, 6682–6690.
2 P. Gupta, K. Vermani and S. Garg, Drug Discov. Today, 2002, 7, 569–579.
3 K. Y. Lee and D. J. Mooney, Chem. Rev., 2001, 101, 1869–1879.
4 M. Kokabi, M. Sirousazar and Z. M. Hassan, Eur. Polym. J., 2007, 43, 773–781.
5 F. Ganji, S. Vasheghani-Farahani and E. Vasheghani-Farahani, Iran. Polym. J., 2010, 19, 375–398.
6 C. J. Bettinger, J. P. Bruggeman, J. T. Borenstein and R. S. Langer, Biomaterials, 2008, 29, 2315–2325.
7 M. C. Koetting, J. T. Peters, S. D. Steichen and N. A. Peppas, Mater. Sci. Eng. R Reports, 2015, 93, 1–49.
8 J. Zhu and R. E. Marchant, Expert Rev. Med. Devices, 2011, 8, 607–626.
9 M. Frydrych, S. Román, N. H. Green, S. MacNeil and B. Chen, Polym. Chem., 2015, 6, 7974–7987.
10 I. El-Sherbiny and M. Yacoub, Glob. Cardiol. Sci. Pract., 2013, 2013, 316–42.
11 M. Ebara, Y. Kotsuchibashi, R. Narain, N. Idota, Y.-J. Kim, J. M. Hoffman, K. Uto and T. Aoyagi, in Smart Biomaterials, Springer Japan, 2014, p. 9.
12 Y. Wang, G. A. Ameer, B. J. Sheppard and R. Langer, Nat. Biotechnol., 2002, 20, 602–606.
13 M. Frydrych, S. Román, S. Macneil and B. Chen, Acta Biomater., 2015, 18, 40–49.
14 R. Rai, M. Tallawi, N. Barbani, C. Frati, D. Madeddu, S. Cavalli, G. Graiani, F. Quaini, J. A. Roether, D. W. Schubert, E. Rosellini and A. R. Boccaccini, Mater. Sci. Eng. C, 2013, 33, 3677–3687.
15 R. Ravichandran, J. R. Venugopal, S. Sundarrajan, S. Mukherjee, R. Sridhar and S. Ramakrishna, Nanotechnology, 2012, 23, 385102.
16 Q. Z. Chen, A. Bismarck, U. Hansen, S. Junaid, M. Q. Tran, S. E. Harding, N. N. Ali and A. R. Boccaccini, Biomaterials, 2008, 29, 47–57.
17 J. M. Kemppainen and S. J. Hollister, J. Biomed. Mater. Res. - Part A, 2010, 94, 9–18.
18 C. G. Jeong and S. J. Hollister Scott J., Biomaterials, 2010, 31, 4304–4312.
19 C. A. Sundback, J. Y. Shyu, Y. Wang, W. C. Faquin, R. S. Langer, J. P. Vacanti and T. A. Hadlock, Biomaterials, 2005, 26, 5454–5464.
20 W. L. Neeley, S. Redenti, H. Klassen, S. Tao, T. Desai, M. J. Young and R. Langer, Biomaterials, 2008, 29, 418–426.
21 C. D. Pritchard, K. M. Arnér, R. A. Neal, W. L. Neeley, P. Bojo, E. Bachelder, J. Holz, N. Watson, E. A. Botchwey, R. S. Langer and F. K. Ghosh, Biomaterials, 2010, 31, 2153–2162.
22 J. Gao, P. Crapo, R. Nerem and Y. Wang, J. Biomed. Mater. Res. - Part A, 2008, 85, 1120–1128.
23 P. M. Crapo, J. Gao and Y. Wang, J. Biomed. Mater. Res. - Part A, 2008, 86, 354–363.
24 D. Motlagh, J. Yang, K. Y. Lui, A. R. Webb and G. A. Ameer, Biomaterials, 2006, 27, 4315–4324.
25 I. Pomerantseva, N. Krebs, A. Hart, C. M. Neville, A. Y. Huang and C. A. Sundback, J. Biomed. Mater. Res. - Part A, 2009, 91, 1038–1047.
26 Y. Wang, Y. M. Kim and R. Langer, J. Biomed. Mater. Res., 2003, 66, 192–197.
27 Z. You, H. Cao, J. Gao, P. H. Shin, B. W. Day and Y. Wang, Biomaterials, 2010, 31, 3129–3138.
28 R. Maliger, P. J. Halley and J. J. Cooper-White, J. Appl. Polym. Sci., 2013, 127, 3980–3986.
29 D. Kafouris, F. Kossivas, C. Constantinides, N. Q. Nguyen, C. Wesdemiotis and C. S. Patrickios, Macromolecules, 2013, 46, 622–630.
30 X. Li, A. T. L. Hong, N. Naskar and H. J. Chung, Biomacromolecules, 2015, 16, 1525–1533.
31 Y. Li, W. D. Cook, C. Moorhoff, W. C. Huang and Q. Z. Chen, Polym. Int., 2013, 62, 534–547.
32 A. Patel, A. K. Gaharwar, G. Iviglia, H. Zhang, S. Mukundan, S. M. Mihaila, D. Demarchi and A. Khademhosseini, Biomaterials, 2013, 34, 3970–3983.
33 L. Zhou, H. He, C. Jiang and S. He, J. Appl. Polym. Sci., 2015, 132, 42196.
34 M. Tallawi, R. Rai, M. R-Gleixner, O. Roerick, M. Weyand, J. A. Roether, D. W. Schubert, A. Kozlowska, M. El Fray, B. Merle, M. Göken, K. Aifantis and A. R. Boccaccini, Macromol. Symp., 2013, 334, 57–67.
35 H. J. Chung and T. G. Park, Adv. Drug Deliv. Rev., 2007, 59, 249–262.
36 Q.-Y. Liu, S.-Z. Wu, T.-W. Tan, J.-Y. Weng, L.-Q. Zhang, L. Liu, W. Tian and D.-F. Chen, J. Biomater. Sci. Polym. Ed., 2009, 20, 1567–1578.
37 Y. Wu, L. Wang, B. Guo and P. X Ma, J. Mater. Chem. B, 2014, 2, 3674–3685.
38 H. Ye, C. Owh and X. J. Loh, RSC Adv., 2015, 5, 48720–48728.

View Article Online
DOI: 10.1039/C8PY00544C

39 P. Aramwit, N. Jaichawa, J. Ratanavaraporn and T. Srichana, Mater. Express, 2015, 5, 241–248.
40 A. O. Elzoghby, J. Control. Release, 2013, 172, 1075–1091.
41 A. P. Kishan, R. M. Nezarati, C. M. Radzicki, A. L. Renfro, J. L. Robinson, M. E. Whitely and E. M. Cosgriff-Hernandez, J. Mater. Chem. B, 2015, 3, 7930–7938.
42 A. Sharma, S. Bhat, T. Vishnoi, V. Nayak and A. Kumar, Biomed Res. Int., 2013, 2013, 478279.
43 M. Tamura, F. Yanagawa, S. Sugiura, T. Takagi, K. Sumaru and T. Kanamori, Sci. Rep., 2015, 5, 15060.
44 M. E. Hoque, T. Nuge, T. K. Yeow, N. Nordin and R. G. S. V Prasad, Polym. Res. J., 2015, 9, 15–32.
45 K. Yue, G. Trujillo-de Santiago, M. M. Alvarez, A. Tamayol, N. Annabi and A. Khademhosseini, Biomaterials, 2015, 73, 254–271.
46 J. Ma, H. Cao, Y. Li and Y. Li, J. Biomater. Sci. Polym. Ed., 2002, 13, 67–80.
47 M. Frydrych and B. Chen, J. Mater. Chem. B, 2013, 1, 6650–6661.
48 J. S. Barbieri, D. J. Margolis and B. A. Brod, J. Invest. Dermatol., 2017, 137, 2491–2496.
49 T. Hattori, R. Hallberg and P. L. Dubin, Langmuir, 2000, 16, 9738–9743.
50 T. R. Anderson, M. E. Marquart and A. V. Janorkar, J. Biomed. Mater. Res. - Part A, 2015, 103, 782–790.
51 Y. Murawaki, H. Kawasaki and H. Burkhardt, Pathol. Res. Pract., 1994, 190, 929–33.
52 J. S. Chawla and M. M. Amiji, Int. J. Pharm., 2002, 249, 127–138.
53 W. Cai and L. Liu, Mater. Lett., 2008, 62, 2175–2177.
54 Q. Liu, M. Tian, R. Shi, L. Zhang, D. Chen and W. Tian, J. app, 2007, 104, 1131–1137.
55 A. Rodriguez-Galan, L. Franco and J. Puiggali, Polymers, 2011, 3, 65–99.
56 T.-H. Nguyen and B.-T. Lee, J. Biomed. Sci. Eng., 2010, 3, 1117–1124.
57 O. Dragostin, S. Samal, F. Lupascu, A. Pânzariu, P. Dubruel, D. Lupascu, C. Tuchilus, C. Vasile and L. Profire, Int. J. Mol. Sci., 2015, 16, 29843–29855.
58 E. A. Kamoun, X. Chen, M. S. Mohy Eldin and E. R. S. Kenawy, Arab. J. Chem., 2015, 8, 1–14.
59 J. T. Bamgbose, A. A. Bamigbade, S. Adewuyi, E. O. Dare, A. A. Lasisi and A. N. Njah, J. Chem. Chem. Eng., 2012, 6, 272–283.
60 E. M. Davis, M. Minelli, M. G. Baschetti and Y. A. Elabd, Ind. Eng. Chem. Res., 2013, 52, 8664–8673.
61 S. B. Tiwari and A. R. Rajabi-Siahboomi, in Drug Delivery Systems, eds. K. K. Jain and J. M. Walker, Springer Science & Business Media, Totowa, NJ, 2008, p. 224.
62 E. P. Holowka and S. K. Bhatia, in Drug Delivery: Materials Design and Clinical Perspective, Springer Science & Business Media, New York, NY, 2014, p. 8.
63 G. Aguirre-Alvarez, D. J. Pimentel-Gonzalez, R. G. Campos-Montiel, T. Foster and S. E. Hill, CYTA J. Food, 2011, 9, 243–249.
64 G. Ninan, J. Joseph and Z. Abubacker, J. Food Sci., 2010, 75, 620–626.
65 Y. Tsuda, in Polyimides and Other High Temperature Polymers: Synthesis, Characterization and Applications, Volume 5, ed. K. L. Mittal, CRC Press, Boca Raton, FL, 2009, p. 26.
66 J. A. Moore and W. W. Bunting, in Advances in Polymer Synthesis, Volume 31, eds. B. M. Culbertson and J. E. McGrath, Plenum Press, New York, NY, 1985, p. 69.
67 K. Pal, A. K. Banthia and D. K. Majumdar, AAPS PharmSciTech, 2007, 8, E142–E146.
68 R. S. H. Wong, M. Ashton and K. Dodou, Pharmaceutics, 2015, 7, 305–319.
69 A. D. Lantada, E. C. Mayola, S. Deschamps, B. P. Sánchez, J. P. G. Ruíz and H. A. Iniesta, in Microsystems for Enhanced Control of Cell Behavior: Fundamentals, Design and Manufacturing Strategies, Applications and Challenges, ed. A. D. Lantada, Springer, Cham, 2016, p. 306.
70 H. Park, B. L. Larson, M. D. Guillemette, S. R. Jain, C. Hua, G. C. Engelmayr and L. E. Freed, Biomaterials, 2011, 32, 1856–1864.
71 S. J. Hollister, Nat. Mater., 2006, 4, 518–524.
72 V. V. Khutoryanskiy, Nat. Mater., 2015, 14, 963–964.
73 D. F. Evans, G. Pye, R. Bramley, A. G. Clark, T. J. Dyson and J. D. Hardcastle, Gut, 1988, 29, 1035–41.
74 E. Osti, Ann. Burns Fire Disasters, 2008, 21, 73–7.
75 J. P. D. Garcia, M. F. Hsieh, B. T. Doma, D. C. Peruelo, I. H. Chen and H. M. Lee, Polymers, 2014, 6, 39–58.
76 S. Riedel, B. Heyart, K. S. Apel and S. G. Mayr, Sci. Rep., 2017, 7, 2–7.
77 Azizullah, Nisar-ur-Rehman, W. Liu, A. Haider, U. Kortz, M. Sohail, S. A. Joshi and J. Iqbal, Des. Monomers Polym., 2016, 19, 697–705.
78 Y. Liu, X. Fan, B. Wei, Q. Si, W. Chen and L. Sun, Int. J. Pharm., 2006, 308, 205–209.
79 L. Liu, W. Yao, Y. Rao, X. Lu and J. Gao, drug Deliv., 2017, 24, 569–581.
80 Q. Chen, X. Yang and Y. Li, RSC Adv., 2012, 2, 4125–4134.
81 M. Biondi, F. Ungaro, F. Quaglia and P. A. Netti, Adv. Drug Deliv. Rev., 2008, 60, 229–242.
82 F. J. O'Brien, Mater. Today, 2011, 14, 88–95.
83 J. S. Boateng, K. H. Matthews, H. N. E. Stevens and G. M. Eccleston, J. Pharm. Sci., 2008, 97, 2892–2923.
84 P. X. Ma, Mater. Today, 2004, 7, 30–40.
85 N. A. Liechty, W. B., Kryscio, D.R., Slaughter, B. V. and Peppas, Annu. Rev. Chem. Biomol. Eng., 2010, 1, 149–173.
86 Z. J. Sun, C. Chen, M. Z. Sun, C. H. Ai, X. L. Lu, Y. F. Zheng, B. F. Yang and D. L. Dong, Biomaterials, 2009, 30, 5209–5214.

View Article Online
DOI: 10.1039/C8PY00544C

Synthesis and biomedical applications of novel elastomeric, pH-responsive, biocompatible and biodegradable copolymer hydrogels based on poly(glycerol sebacate) and gelatin